

# Chapter 7

## 3D dynamical system

### 7.1 Introduction

In this chapter a low-dimensional dynamical system for the flow in a 3D driven cavity is discussed. In Section 7.2 we discuss some implication of the symmetries in the eigenfunctions for the coefficients in the dynamical system. Also the model for the non-retained eigenfunctions in the dynamical system is discussed. The short- and long-time integrations of the dynamical system at  $Re=10,000$  are presented in Section 7.3. We have used 80 eigenfunctions in the dynamical system. These 80 eigenfunctions possess on average 62% of the fluctuating energy. This is far less than the energy content of the first 80 eigenfunctions in 2D. Indeed, in two dimensions the first 80 eigenfunctions possess more than 95% and the first 10 contain 62% of the fluctuating energy. A second remarkable difference is the percentage of the fluctuating energy as part of the total energy. This percentage is considerably smaller in 2D than in 3D: 1.2% against 9%. Consequently it is likely that the 3D 80-dimensional dynamical system performs worse than 2D 80-dimensional dynamical system. In 3D we could not use more than 80 POD eigenfunctions in the construction of the dynamical system, since the computation of the dynamical system becomes too expensive for more than 80 eigenfunctions. In addition, the time integration of the dynamical system would be far more expensive, because the computation time for time integration of the dynamical system is proportional to the third power of the number of eigenfunctions.

Section 7.4 describes the behavior of the dynamical system at Reynolds numbers different than  $Re=10,000$ , i.e. the Reynolds number at which the dynamical system is constructed. We have found that the transition behavior of the dynamical system differs from the transition behavior which is found by experiments and DNS (see [1, 42, 62]).

Finally in Section 7.5 conclusions will be drawn.

### 7.2 Low-dimensional dynamical system

The system of ordinary differential equations for the coefficients  $a^k$  is given by equation (5.1). Here 50% of the terms are zero due to the symmetry of the eigenfunctions: the  $L^2$ -innerproduct of an odd and an even function is zero, derivatives of eigenfunctions are

either odd or even, and the mean flow is even. Therefore, 50% of terms in the dynamical system are zero.

In particular the terms  $C_k$  (see (2.39)) in the differential equation for an odd eigenfunction are zero. If all coefficients of all odd eigenfunctions are zero, also all the other terms in the differential equation for an odd eigenfunction are zero. So, if the initial flow is even it stays even for all times. This is what we would expect for a flow geometry with such a symmetry. This symmetric flow, however, is not stable with respect to small disturbances.

For the 3D dynamical system we have used the linear damping model which has been introduced in Section 2.5, since this model performed the best of the models that are used in Section 5.3. In addition, it does not require trial-and-error for the determination of the adjustable constant.

In 3D we have modified the coefficient  $1/Re$  as in 2D (see Section 5.2.1). The result is shown in Fig. 7.1.

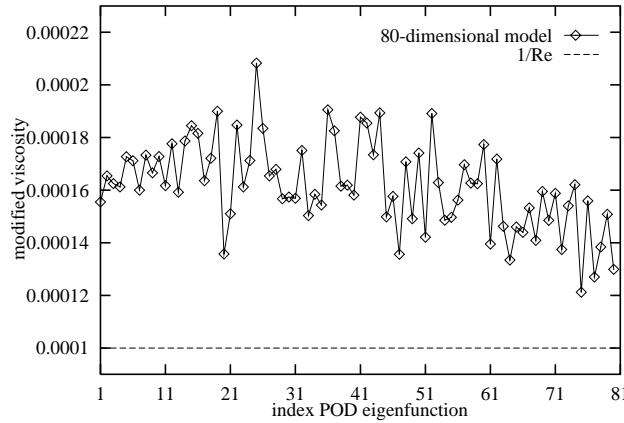


Figure 7.1: *The modified viscosity for the linear damping model as a function of the index of the POD eigenfunction.*

We can see that, unlike in 2D, the modified coefficients are all larger than  $1/Re$ . This is an indication that we capture only large scales with 80 eigenfunctions, and no small (dissipative) scales. Indeed, the eigenfunctions with an index larger than 80 subtract energy (on average) from the first 80 eigenfunctions.

## 7.3 Dynamical system at $Re=10,000$

### 7.3.1 Short-time integrations

We have performed short-time integrations to verify the convergence of the dynamical system to the DNS when more POD eigenfunctions are retained in the dynamical system.

The results are shown in Fig. 7.2. Just like in the 2D case we have started all integrations from an arbitrary velocity field projected on the first 20 eigenfunctions. The left

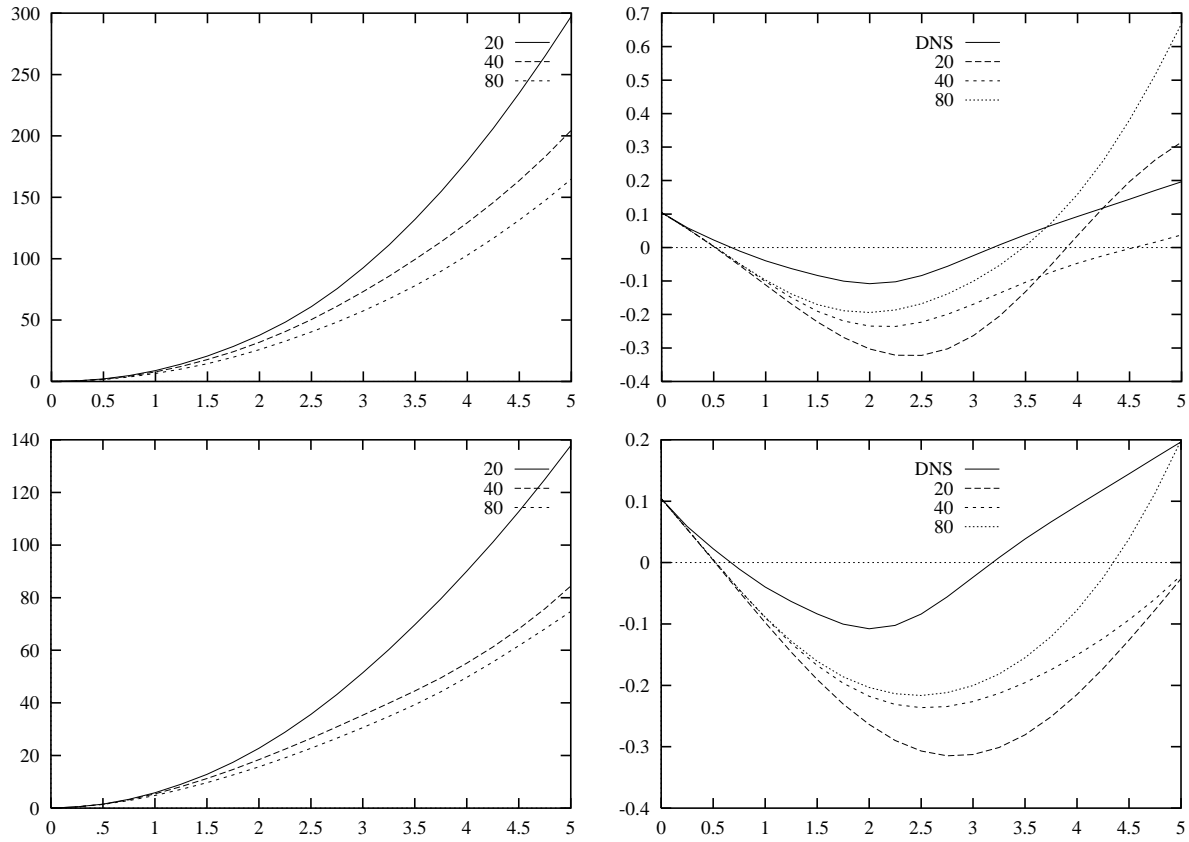


Figure 7.2: *The convergence of the low-dimensional dynamical system to the DNS as a function the number of POD eigenfunctions. In every plot the results of the dynamical system with 20, 40, and 80 POD eigenfunctions are shown. Left the sums of the deviations from the DNS of the first 20 coefficients integrated in time and right the coefficients of the first eigenfunction during the first 5 time units are shown. On top the dynamical system with no model is shown; in the lower two plots the linear damping model has been used.*

plots of Fig. 7.2 shows that the more eigenfunctions are retained, the closer the coefficients stay to the DNS coefficients. The dynamical system without a model deviates much faster and further from the DNS than the dynamical system with a linear viscosity model. Moreover, the dynamical system without a model converges to a statistical equilibrium around a non-physical solution.

The right-hand plots of Fig. 7.2 show the coefficients during 5 time units. We can see that the 3D driven cavity at  $Re=10,000$  has a different characteristic time-scale than the 2D driven cavity at  $Re=22,000$  (see Fig. 5.2). With the linear damping model the 80-dimensional dynamical system stays the closest to the DNS.

### 7.3.2 Long-time integrations

For the long-time integrations we have also used the model with linear damping. We have integrated the dynamical system for 800 time units, that is as long as the DNS simulation which produced the snapshots for the POD. The results are shown in Fig. 7.3.

The left plot shows the fluctuating energy. For a fair comparison with the DNS

we should compare the energy of the snapshots after they are projected on the first 80 eigenfunctions. This energy is shown in Fig. 7.4. The energy signal of Fig. 7.4 looks like the energy of the unprojected snapshots as shown in Fig. 3.13. The difference is that the level of the energy shown in Fig. 7.4 is approximately 60% of the level of the energy in Fig. 3.13. This friction is in agreement with the energy content (62%) of the first 80 eigenfunctions (see Table 6.1).

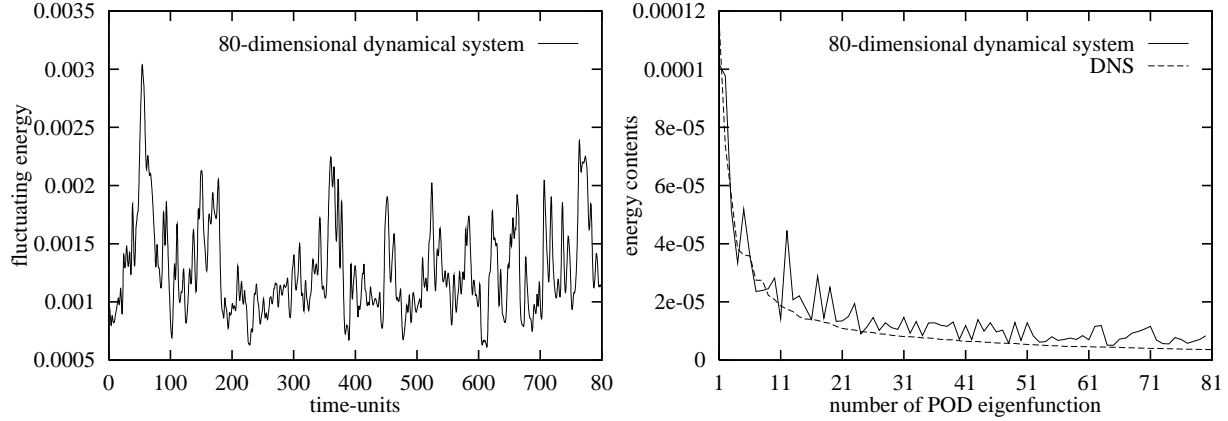


Figure 7.3: *Fluctuating energy and spectrum of the 80-dimensional dynamical system with the linear eddy viscosity model.*

The fluctuating energy of the dynamical system is shown in Fig. 7.3 (left). It has higher peaks than the fluctuating energy of the DNS (see Fig. 7.4). The energy content (shown in Fig. 7.3 on the right-hand) as a function of the number of POD eigenfunctions is fairly close to the DNS. Some eigenfunctions (especially the one with index 12) have too much energy. The energy content of the tail of the spectrum is systematically too high.

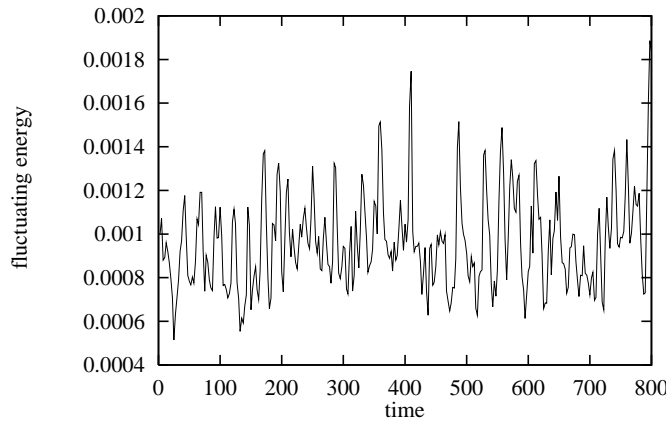


Figure 7.4: *Energy of the snapshots projected on the first 80 POD eigenfunctions.*

We have also compared the root-mean-square (rms) values of the  $u$ - and  $v$ -velocities and the Reynolds shear stresses (see Fig. 3.15). A property of the POD, as presented

in Chapter 2, is that the correlation coefficient of  $a^i$  and  $a^j$  is zero if  $i \neq j$ . The long-time integrations of the 80-dimensional dynamical system with the linear damping model yield non-zero cross-correlation coefficients. These cross-correlations have, even if they are relatively small, a large influence on both the rms values and Reynolds shear stresses, since there are 6320 cross-correlation coefficients and only 80 auto-correlation coefficients. We have compared the results of the experiments of Prasad and Koseff [42] and the DNS with the results of the dynamical system where we neglect the cross-correlations, i.e. we only have taken the auto-correlation into account.

From the DNS we know that the Reynolds shear stresses converge slowly and that they are relatively small compared to the rms values. We have found that the resemblance between the dynamical system and the DNS- and experimental results is not very good. The Reynolds shear stresses of the dynamical system are too low. Maybe this is due to the fact that the first 80 eigenfunctions contain only 62% of the energy.

We have also compared the rms values. The results are shown in Fig. 7.5. We can see that the  $u_{rms}$ -value of the dynamical system is too low, but that the  $v_{rms}$ -value of the dynamical system approximates the DNS- and experimental values very good in the  $x=1$  area. This indicates that the POD eigenfunctions do approximate the energy very well (at  $x=1$  the energy is approximately  $v^2$ ). It may be noted that the POD eigenfunctions have high energetic structures in the DP location.

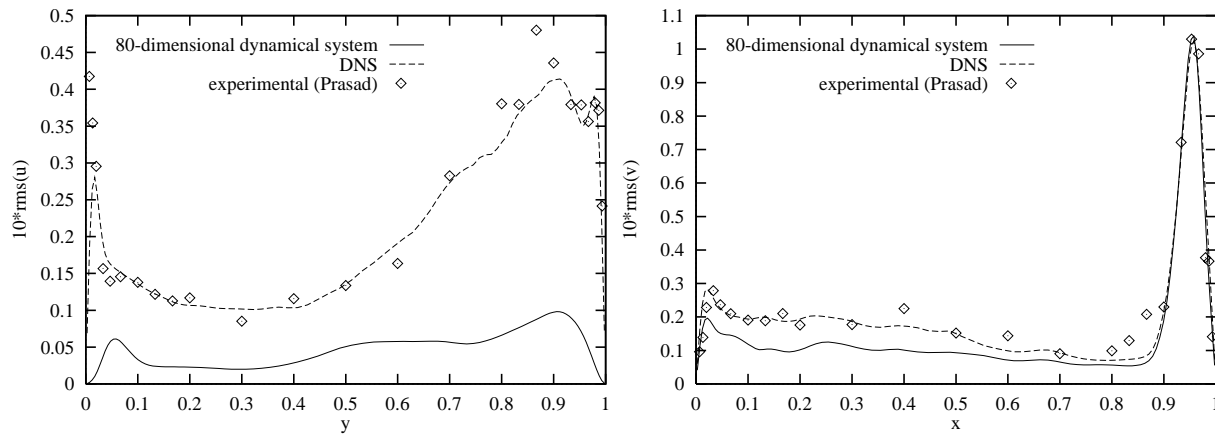


Figure 7.5: Comparison of the root-mean-square value of the  $u$ - and  $v$ -velocity of the DNS and of the 80-dimensional dynamical system. The left-hand plot shows  $u_{rms}$  along the vertical line through the center of the cavity (the upper lid is  $y=0$  in this plot); The right-hand plot shows the  $v_{rms}$  along the horizontal line through the center of the cavity in the  $x$ -direction.

## 7.4 Transition

The experiments of Prasad and Koseff reveal that the flow in a 3D driven cavity is already unstable at  $Re=3,200$ . Numerical experiments of Freitas *et al.* [19] at the same Reynolds number reproduced the experimentally observed Taylor-Görtler vortices.

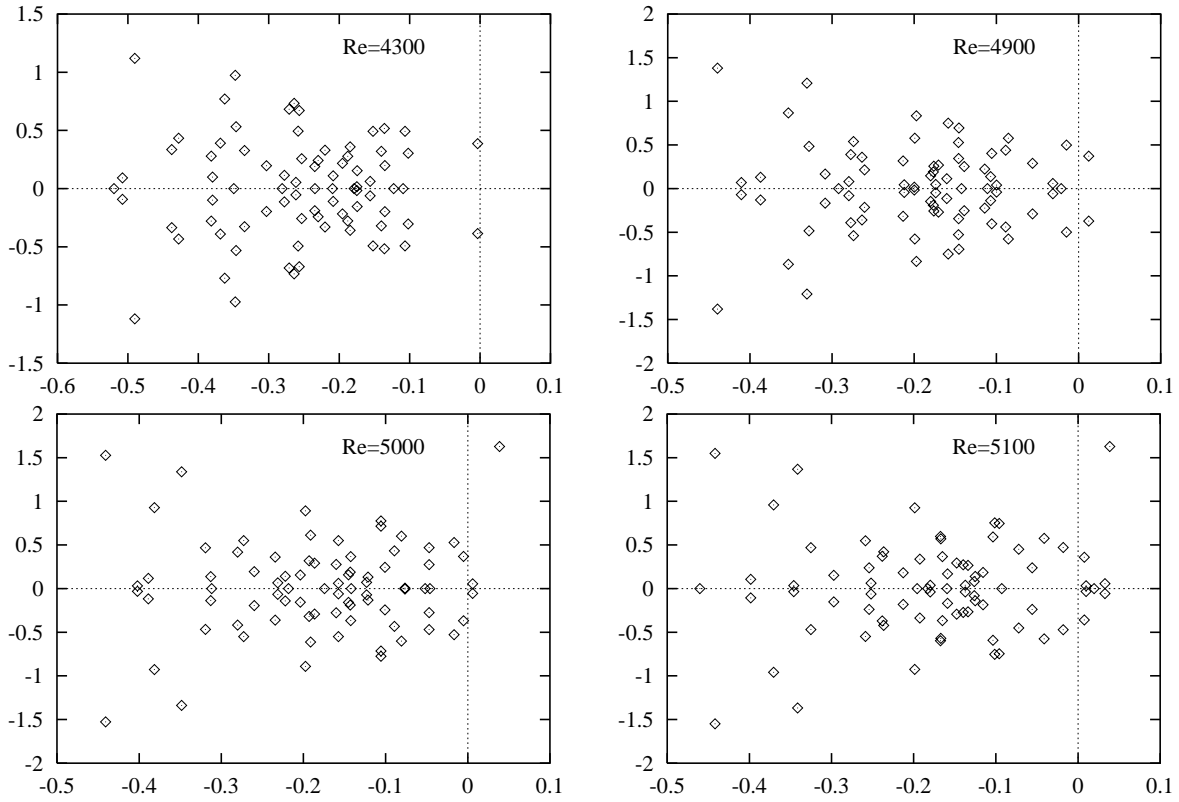


Figure 7.6: *Eigenvalues in the complex plane of the Jacobian of the equations for the steady-state solution at Reynolds numbers 4300, 4900, 5000, and 5100.*

DNS of a 3D driven cavity with periodic boundary conditions (see Wissink [62]) showed that (Taylor-Görtler-like) vortices emerge somewhere between  $Re=700$  and  $Re=800$ . At  $Re=3,200$  Wissink found that the flow is unsteady. Aidun *et al.* [1] have presented experimental results of a periodic flow in a lid-driven cavity with through-flow at  $Re=825$ .

The 80-dimensional dynamical system has a steady state solution until approximately  $Re=4,300$ . Just after this Reynolds number the first (Hopf) bifurcation takes place, as is shown in Fig. 7.6. At  $Re=4,900$  other eigenvalues have reached the imaginary axis. At  $Re=5,000$  the pair of eigenvalues that first crossed the imaginary axis returns to the left half-plane, and another pair of eigenvalues enters the right half-plane. At  $Re=5,100$  7 eigenvalues lie in the right half-plane!

The  $Re$ -values at which the first bifurcations take place are much higher for the 80-dimensional dynamical system than for the DNS- and the experiments. In addition, the transition process is very rapid between  $Re=5,000$  and  $Re=5,100$ . The agreement between the 80-dimensional dynamical system and the DNS- and experimental results is too poor to investigate the transition of the dynamical system in detail.

Possible causes for this poor agreement are (i) the low energy content of the first 80 POD eigenfunction, and (ii) the fact that the mean flow at  $Re=10,000$  (which captures 90% of the total energy of the solution of the dynamical system) is quite different from the mean flow at low ( $\sim 1,000$ ) Reynolds numbers.

## 7.5 Conclusions

In this chapter we have presented results for the dynamical system for the 3D driven cavity flow. They lead to the following conclusions.

- The short-time integrations showed that the dynamical system results converge to the DNS results as the number of snapshots increases.
- For long-time integration the energy-spectrum of the dynamical system could be reproduced reasonably well. In addition, the  $v_{rms}$ -value at the DP as predicted by the 80-dimensional dynamical system approximates the DNS- and experimental value well.
- The transition of the dynamical system is in poor agreement with the transition observed in DNS and experiments.

# Conclusions

The main subject of this thesis was the investigation of the performance of a low-dimensional dynamical system in describing turbulent flows in driven cavities. We derived this low-dimensional dynamical system via a Galerkin projection of the Navier-Stokes equation on a set of functions: the so-called POD eigenfunctions. These POD eigenfunctions are eigenfunctions of the space-correlation tensor.

The POD eigenfunctions have properties which lead to the expectation that they form a suitable basis for a low-dimensional dynamical system. Some of these properties were presented in Chapter 2. The most important is the maximum energy content of the POD eigenfunctions. It means that the first  $N$  POD eigenfunctions contain more energy (on average) than every other set of  $N$  functions.

For the computation of the POD eigenfunctions we used the so-called snapshot method of Sirovich. They are supplied by a direct numerical simulation (DNS). With the DNS we found that the 2D driven cavity at  $Re=22,000$  has a long time-scale which corresponds to the building up of energy in a large eddy in the core of the cavity followed by the dissipation of that energy by the entrance of smaller vortex-structures from the corners into the core region of the cavity.

Furthermore, our DNS computations showed that the flow in a 2D driven cavity undergoes a Hopf bifurcation at approximately  $Re=7,972$ . This is in contradiction with the steady flows in driven cavities at  $Re=10,000$  which have been reported in many papers. A popular reference is [20]. The value of  $Re=7,972$  lies close to the value of  $Re=7,763\pm 2\%$  given by Poliashenko and Aidun [41] for the first bifurcation. Our computations showed that even a second bifurcation has taken place for  $Re<10,000$ , which is in agreement with the results of Liffman [31]. Because the flow in a driven cavity is often used as a reference for new simulation methods, it is important to know the solution. Our results clearly show that the first bifurcation takes place before  $Re=8,000$ , and that the solution at  $Re=10,000$  has 2 frequencies.

Another interesting outcome of the DNS computation is the finding of stable 1-periodic solutions in the range  $Re=12,000-16,000$ . At  $Re=16,000$  we found, beside this 1-periodic solution, also a solution with at least two different frequencies.

In Chapter 4 we presented results of the POD eigenfunctions computation of the 2D driven cavity flow at  $Re=22,000$ . We verified that with 700 snapshots the eigenvalues corresponding the POD eigenfunctions are more or less converged. The high energetic eigenfunctions, however, converge faster than their corresponding eigenvalues. Therefore it is reasonable to expect that our POD eigenfunctions are close to the "real" POD eigenfunctions. The properties of these "snapshot" POD eigenfunctions are the same as for the "real" eigenfunctions when we consider only the set of 700 snapshots.



The main conclusions which can be drawn from the computed POD eigenfunctions are: the high energetic eigenfunctions contain large flow structures, most energy (of the fluctuations) is present in the lower right corner, the high energetic eigenfunctions can be grouped in pairs and the seventeenth POD eigenfunction has a large eddy in the core region of the cavity just like the mean flow. In addition to this last conclusion we showed that the coefficient of the seventeenth POD eigenfunction also has a long time-scale corresponding to the long time-scale of the DNS. From this we can conclude that for the dynamical behavior of the flow also (relatively) low-energetic flow structures can be important. This poses an important question for constructing low-dimensional models for turbulent flows via a Galerkin projection on steady modes: how can we choose dynamically important basisfunctions? We will refer to this question in the suggestions for further research below.

In Chapter 4 results of the 80-dimensional dynamical system for the flow in a 2D driven cavity are reported. An important conclusion is that it is necessary for doing long time-integrations to use a model for the interaction between the resolved and non-resolved eigenfunctions. We got the best results with a model based on the average energy exchange between the eigenfunctions, although the dynamics responsible for the long time-scale of the DNS could not be accurately reproduced by this model. This is probably due to the fact that the snapshots used to compute the POD eigenfunctions have a low resolution of a vortex-structure dissipating in the core of the cavity. On the other hand, it would be questionable if the first 80 POD eigenfunctions computed with an 'infinite' number of snapshots would be able to represent accurately a moving vortex-structure in the core of the cavity.

We used the POD eigenfunctions computed at  $Re=22,000$  for an analysis of the first bifurcations of the flow in a 2D driven cavity. The Reynolds number at which the first (Hopf) bifurcation takes place ( $Re=7,819$ ) lies close to the value of the DNS ( $Re=7,972$ ). The periods of the periodic solutions are, however, different.

With Floquet analysis we found in the range  $Re=11,188$ - $11,500$  2-periodic solutions the ratio of which is approximately the same as the ratio of the two periods of the 2-periodic solution of the DNS at  $Re=11,000$ . The 2-periodic solution of the dynamical system bifurcates again to a stable 1-periodic solution at approximately  $Re=11,500$ . For the DNS we found also a 1-periodic solution at  $Re=12,000$ . The periodic solutions of the dynamical system at  $Re=11,800$  and the DNS at  $Re=12,000$  have approximately the same period and have qualitatively the same behavior. We can conclude that we clearly found similarities in dynamical behavior between the low-dimensional dynamical system and the DNS, but the transition is not the same.

For the 3D driven cavity flow we used 320 snapshots to compute the POD. We used the symmetry plane at  $z=0.5$  to enlarge the database and to force the eigenfunction to be odd or even with respect to the symmetry plane. We found that the high energetic eigenfunctions were formed with a low number of snapshots but the energy of these eigenfunctions changed. So the high-energetic eigenfunctions can be formed with a relatively small number of snapshots.

The first POD eigenfunctions showed Taylor-Görtler like vortices as has been observed experimentally by Prasad and Koseff [42] at lower Reynolds numbers. Moving vortices in spanwise direction can be represented by a linear combination of the POD eigenfunctions. This spanwise motion of vortices have also been observed in experiments (at lower

Reynolds numbers).

Most of the POD eigenfunctions showed an oscillating behavior of the  $v$ - and  $w$ -velocities in the  $z$ -direction close to the wall at  $x=1$  indicating that the flow is more or less homogeneous in that direction.

The relative energy content of the first 80 POD eigenfunctions for the 3D driven cavity was lower than the relative energy content of the 2D driven cavity. In addition the energy of the fluctuations in the 3D case was higher than in the 2D case (9.0% versus 1.2% of the total kinetic energy). Therefore, we expected less resemblance between the 3D 80 dimensional dynamical system and the 3D DNS than in the corresponding 2D case.

The short-time integrations of the dynamical system derived with 80 POD eigenfunctions showed that the dynamical system results converge to the DNS results as the number of snapshots increased. For the long-time integration the energy-spectrum of the dynamical system could be reproduced reasonably well. In addition, the  $v_{rms}$ -value close to the wall at  $x=1$  as predicted by the 80-dimensional dynamical system approximates well the DNS- and experimental value. The transition of the dynamical system is in poor agreement with the transition observed in DNS and experiments.

## Suggestions for further research

One of the great difficulties in computing the POD eigenfunctions is the large amount of data which is necessary. One technique to enlarge the database at small costs is to make use of the symmetries of the flow geometry, a method which we applied for the 3D driven cavity. Another possibility is to use a lower resolution for the snapshots than the resolution used in the DNS. We expect that this will not effect the high energetic POD eigenfunctions too much, because the high energetic eigenfunctions represent large scale structures which can be represented with a lower resolution. This will resolve for a large part the difficulties we had with handling the large amount of DNS data.

Another problem which will need attention is the increase of computing time by increasing the number of POD eigenfunctions. The computing time is proportional to the third power of the number of eigenfunctions (independent of the dimension!). It would be worthwhile to investigate the coupling of POD eigenfunction for the large scale, and Fourier modes for the small scales (which are more homogeneous) for which we can use the Fast Fourier Transform.

One of the possible causes for the differences between the transition behavior of the low-dimensional dynamical system and the transition behavior of the DNS is the dependence of the POD eigenfunctions on the flow and thus on the Reynolds number. The POD eigenfunctions computed at  $Re=22,000$  do not capture a maximum energy at other Reynolds numbers. Also the mean flow can have a different flow-pattern at other Reynolds numbers. For transition analysis it is necessary that the solution at other Reynolds number can be reasonably approximated with a linear combination of the POD eigenfunctions added to the mean flow. To make this possible additional functions can be added to the set of POD eigenfunctions used in the Galerkin projection. These additional functions are the difference between the mean flow at  $Re=22,000$  and flowfields at other Reynolds numbers. This has been successfully applied for the flow in a cylinder by Christensen *et al.* [13] (for a POD at a low Reynolds number). A drawback of this method is that the

orthogonality of the extended set of eigenfunctions is lost. An alternative is to use the mean of the extended set of snapshots and compute new eigenfunctions. In that case we retain the orthogonality, but we lose some other properties, and the new computation of the new eigenfunctions is expensive.

A possible answer to the important question from the previous section about dynamically important modes is given by Sirovich. He proposed to search for functions that are optimal in the sense that they minimize the error made by truncating the dynamical system to  $N$  degrees of freedom. These functions appear to be the eigenfunctions of the space-correlation tensor of the accelerations instead of the velocities. This would be an interesting direction for further research.

The span of the POD eigenfunction is a global approximation of the attractor in state space. Another method suggested by Broomhead *et al.* [10] approximates the attractor in state space dynamically. With such a method it is possible to follow a trajectory in state space into an area which is not spanned by the first  $N$  POD eigenfunctions but which is important for the dynamical behavior of the flow. For the 2D driven cavity flow at  $Re=22,000$  this would make it possible to follow the trajectories in state space when a vortex-structure enters the core region of the cavity.

The method of dynamical eigenfunctions introduces a number of difficulties for a high dimensional attractor. A major difficulty is the computational requirements of a dynamical set of eigenfunctions and the Galerkin projection. More research is needed to investigate the feasibility of such a method.